RAPID COMMUNICATIONS

PHYSICAL REVIEW E VOLUME 53, NUMBER 2 FEBRUARY 1996

Measurements of extreme uv opacities in hot dense Al, Fe, and Ho

G. Winhart,[1] K. Eidmann,[1] C. A. Iglesias,[2] and A. Bar-Shalom[3]
[1]*Max-Planck-Institut für Quantenoptik, D-85740 Garching, Germany*
[2]*Lawrence Livermore National Laboratory, L-296, P.O. Box 808, Livermore, California 94550*
[3]*Nuclear Research Center Negev, P.O. Box, Beer Sheva, Israel*
(Received 27 October 1995)

The opacities of aluminum, iron, and holmium were measured spectrally resolved in the energy range of 70 to 280 eV at typical densities and temperatures of about 0.01 g/cm^3 and 22 eV, respectively. For this purpose the iodine laser ASTERIX IV (200 J/0.4 ns at 400 nm) was focused into a spherical gold cavity with a diameter of 3 mm. The generated radiation with a temperature of 60 eV heated thin tampered absorber foils which were probed by the radiation from a backlighter source. The experimental data are compared with theoretical opacity models.

PACS number(s): 52.25.Qt, 52.50.Jm, 44.40.+a, 97.10.Ex

An essential contribution to the energy transport in hot dense plasma is caused by radiation. This is of importance, for example, in astrophysical models of stars [1] or in indirect drive inertial confinement fusion (ICF) targets [2]. Modeling of such plasmas strongly relies on radiative opacities. Theoretical calculations of opacities are very complex and need numerous approximations. Therefore, it is not surprising that different opacity models often differ in their results [3].

To check opacity models, clear measurements at a well defined temperature and density are strongly needed. Recently, such measurements became possible by the technique of radiative heating using the intense thermal x rays emitted by laser-irradiated targets. This method allows uniform volume heating of tampered thin sample foils to temperatures of up to ≈ 100 eV at densities around 0.01 g/cm^3. The opacity is obtained from the transmission of an x-ray probe beam through the heated foil. Many experiments of this type were performed during recent years to study the spectral range at $h\nu \gtrsim 1$ keV by crystal spectroscopy [4–7]. In contrast, the spectral range $h\nu \lesssim 1$ keV is much less explored. It requires reliable extreme uv diagnostics and sufficient suppression of self-emission from the heated sample (or from other sources), which tends to increase in this region. On the other hand, it is this spectral range which determines the Rosseland and Planck mean opacities, i.e., the radiative transport. Experiments in the spectral sub-keV range have recently been performed with iron as the sample material by DaSilva *et al.* [8] at a temperature of ≈ 25 eV in the spectral range 50 eV $\leq h\nu \leq 120$ eV and by Springer *et al.* [9] at a higher temperature of ≈ 59 eV in the spectral range 90 eV $\leq h\nu \leq 300$ eV.

In this paper we present opacity measurements performed with the iodine laser ASTERIX IV at the Max-Planck-Institut für Quantenoptik at $T \approx 22$ eV and $\rho \approx 0.01$ g/cm^3 in the spectral range 70 eV $\leq h\nu \leq 280$ eV. As sample material we used aluminum ($Z=13$), iron ($Z=26$), and holmium ($Z=67$), which elements are considered as representative for low, medium, and high Z. Extreme uv opacity measurements for these parameters have been reported previously only for iron by DaSilva *et al.* [8]. In contrast to this experiment we realized a low level of self-emission which improves the accuracy of the measurement. We emphasize that spectrally resolved extreme uv opacity measurements for high-Z elements such as Ho have not, to our knowledge, been reported previously. The opacity of high-Z elements is of importance for indirect drive ICF where it determines the radiation field building up in high-Z cavities [2], whereas low- or medium-Z elements like Fe are of relevance for astrophysics [1]. The experimental results have been compared with the local thermodynamic equilibrium (LTE) opacity models OPAL and STA.

The scheme of the experimental setup is shown in Fig. 1. To heat the absorber foils we used gold cavities with a diameter of 3 mm which were heated by the main beam of the iodine laser ASTERIX IV (200 J, 0.4 ns, 438 nm). The absorber foils were glued on one of the two diagnostic holes with a diameter of 1 mm which was large enough to prevent hole closing. In addition, we used a Macrofol diaphragm with a diameter of 0.5 mm to suppress edge effects of the diagnostic holes. To reduce axial density gradients due to expansion, we used tampered absorber foils consisting of 560 Å (corresponding to 15 μg/cm^2 areal mass density) carbon on either side of the sample layer. The sample layer was

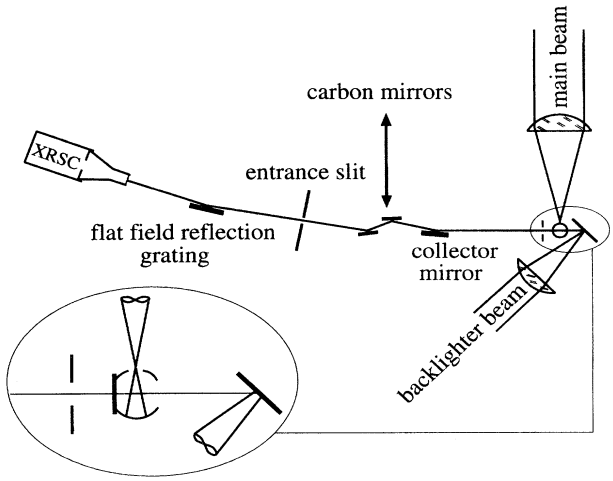

FIG. 1. Scheme of the experimental setup.

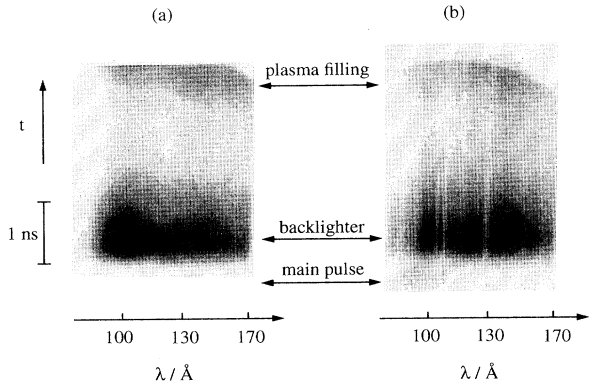

FIG. 2. Streak camera signals of the backlighter observed through a heated cavity (a) without a sample and (b) with an aluminum sample.

either 1075 Å (30 μg/cm^2) thick aluminum or 191 Å (15 μg/cm^2) thick iron or 170 Å (15 μg/cm^2) thick holmium.

A backlighter source was generated by a second laser beam (25 J, 0.4 ns, 1.3 μm), which was focused on a planar gold target with a delay of 800 ps to the main beam. A distance of 1 cm between the backlighter source and the cavity was large enough to prevent heating of the sample by the backlighter. The transmission of the backlighter probe beam through the sample was measured by an extreme uv spectrometer consisting of a collector mirror, which images the source on the entrance slit, a 1200 lines/mm Hitachi flat field reflection grating and an x-ray streak camera as detector [10]. The time resolution was 20 ps and the wavelength resolution 1.0 Å. The absolute wavelength scale has been calibrated by means of line emission spectra with an accuracy of ± 0.5 Å. The probed area of the sample had a diameter of ≈ 300 μm.

Because the flat field grating has a large conversion efficiency into higher diffraction orders, it was necessary to suppress short wavelengths by positioning between the collector mirror and the entrance slit either a thin carbon filter or, alternatively, a set of two parallel flat carbon mirrors. Using the carbon filter, the contributions below 44 Å are suppressed, resulting in a signal which is free of higher orders in the range 44 to 88 Å. The carbon mirrors at 9° grazing angle of incidence eliminate wavelengths below ≈ 85 Å and allow one to record an unperturbed first order spectrum in the range 85 to 170 Å. Thus, in total the wavelength range 44 to 170 Å can be covered.

Figure 2 shows two streak camera records obtained in two different shots. Figure 2(a) is a record of the backlighter spectrum observed through a heated cavity without a sample. The radiation of the plasma filling the cavity appears about 2 ns after the backlighter signal, late enough not to disturb the absorption measurement. Figure 2(b) shows the signal with an aluminum absorber foil on the cavity. Absorption lines of the heated Al appear now. The weak signal seen early at the time of the main beam is attributed to self-emission from the heated sample. Due to the high brightness of the backlighter source the contribution of self-emission from the heated sample does not exceed a few percent of the signal of the absorption spectrum.

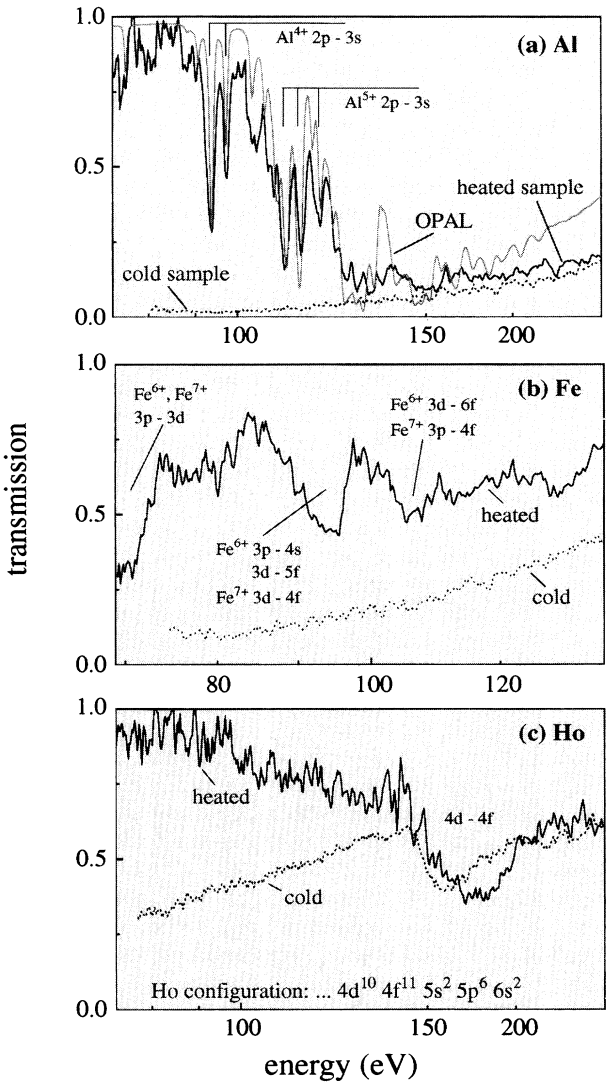

FIG. 3. Measured transmission spectra of (a) aluminum, (b) iron, and (c) holmium for the heated and cold sample, respectively. For Al (a) also a comparison with the OPAL code at $\rho = 0.01$ g/cm^3 and $T = 22$ eV is shown (the OPAL data have been shifted by 3 eV to lower photon energies for an optimum coincidence between the measured and the calculated spectra).

The transmission has been obtained by normalizing the absorption spectrum to the backlighter spectrum. Thus the spectral response of the spectrometer is eliminated. Because the backlighter and absorption spectra were recorded in different shots, small shot to shot variations limited the relative error of the transmission to $\pm 10\%$. Our results obtained for Al, Fe, and Ho are exhibited by Fig. 3. The spectra refer to the time of the maximum of the backlighter pulse and are averaged over a period of 400 ps. (We note that the transmission spectra did not show remarkable changes during the probing time interval of the backlighter.) Correction of the data for the carbon transmission was in most cases not necessary, because it was close to one. Only in case of the Al sample with the larger mass density (30 μg/cm^2 compared to 15 μg/cm^2 used for Fe and Ho) the carbon layer at the rear

side did not completely burn through and a correction was necessary on the long wavelength side of the spectrum. This has been done by using calculated carbon opacities for the density and temperature obtained in hydrodynamic simulations (see below).

By switching off the main beam, we also measured the transmission of the unheated sample. It is plotted in Fig. 3 for comparison with the transmission of the heated sample. The strong influence of the heating on the opacity is well demonstrated. To check the reliability of the experiment we compared the cold data with those compiled by Saloman *et al.* [11]. We find good agreement [12].

We describe now the transmission spectra of the heated samples. Al [Fig. 3(a)] shows several discrete absorption lines. The dominant lines are due to partially resolved $2p$-$3s$ multiplets of Al^{4+} and Al^{5+} indicating an average ionization between 4 and 5. With Fe [Fig. 3(b)] the strongest absorption features are caused by the $3p$-$4s$, $3d$-$5f$ (Fe^{6+}) and $3d$-$4f$ (Fe^{7+}) transition arrays at ≈ 130 Å and the $\Delta n=0$ ($3p$-$3d$) transition array at ≈ 180 Å. Compared to the previous measurement of DaSilva *et al.* [8] at a similar temperature and density, our data are obtained at a much smaller level of self-emission and, therefore, more accurate (for a direct comparison of the two measurements we refer to Ref. [12]). On the other hand, the measurement of DaSilva *et al.* extends to longer wavelengths $\lambda \leq 250$ Å and exhibits the prominent $\Delta n=0$ ($3p$-$3d$) absorption feature in its entirety, including its long wavelength (low energy) side.

In Fig. 3(c) the transmission spectrum of the heated Ho sample is presented. Because of the open $4f$ shell of neutral holmium ($\ldots 4d^{10}4f^{11}5s^25p^66s^2$) the $4d$-$4f$ transition arrays centered at 75 Å can even be observed with cold Ho. In heated Ho with less electrons in the outer shells the $4d$-$4f$ dip is shifted to shorter wavelengths because of less screening by the outer electrons. At the same time, the transparency increases considerably at longer wavelengths because of less photoionization.

For a comparison with opacity models the temperature and density of the samples are needed. For this purpose hydrodynamic simulations have been performed with the MULTI hydrodynamic code [13]. The radiative heating has been modeled by using as the drive radiation Planckian x rays, similarly as has been described in [14]. For the driving Planckian x rays we used a temperature in the range 55 to 60 eV with a pulse duration of 0.5 ns. These values have been inferred from separate measurements of the emission from the inner cavity gold wall by an absolutely calibrated pinhole transmission grating similar to that used previously by us [15]. The simulations yield a maximum temperature of the sample of 40 to 45 eV. At the time of the measurement by the delayed probe beam, the expanding sample foil has cooled down to a temperature of around 20 eV at a density around 0.01 g/cm^3. At this time the spatial temperature variation across the layer of the sample element does not exceed 2 eV.

For these temperatures and densities the state of the plasma is very close to LTE due to the high electron collision rates [12]. Therefore a comparison with the LTE codes OPAL and STA is justified. The OPAL code [16] is developed for low-Z and medium-Z elements such as Fe. It considers the actual multiplet structure by using LS coupling for low-Z (Al) and intermediate coupling for medium-Z (Fe). In contrast, the STA code [17] is appropriate for high-Z elements. It uses the method of super-transition-arrays (STA's) to describe the broad bound-bound structures formed by high-Z elements due to the extremely high line density of the numerous overlapping multiplets.

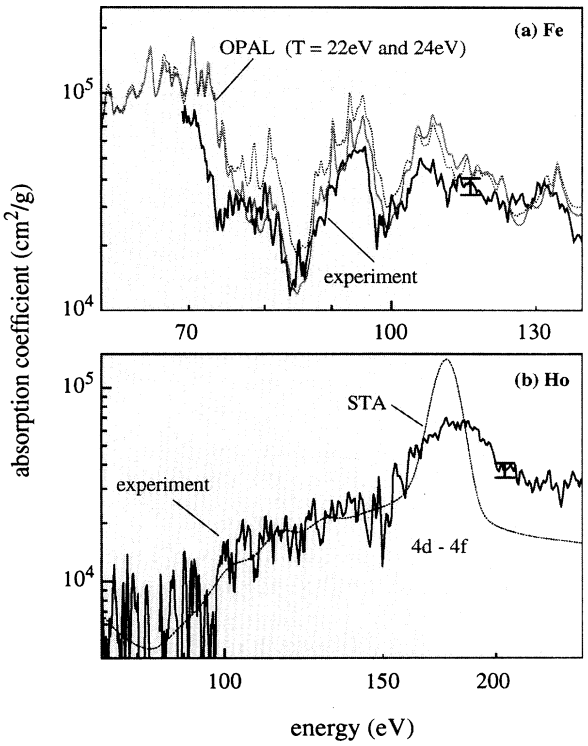

FIG. 4. Measured and calculated mass absorption coefficient versus photon energy for Fe (a) and Ho (b). In the calculations we used for Fe: $\rho=0.01$ g/cm^3 at $T=22$ eV (dotted) and $T=24$ eV (grey); and for Ho: $\rho=0.03$ g/cm^3, $T=20$ eV.

Figure 3(a) shows the comparison of OPAL with the measured Al transmission. The calculated data have been smeared with the experimental spectral resolution. From this comparison, we infer a sample temperature $T=22$ eV for which value the best agreement between theory and measurement is achieved. The accuracy of the temperature obtained by this fit is estimated to be ± 2 eV [12]. The mean ionization calculated by OPAL for this temperature is 4.6 in agreement with the observation that the strongest absorption lines are due to Al^{4+} and Al^{5+}. It is noted that the temperature for the best coincidence does not strongly depend on the assumed density. For example, lowering of the density by a factor of 3 results in a decrease of the temperature by 2 eV to get the same ionization. This type of spectroscopic temperature determination has previously been tested with high accuracy in an Al plasma of similar density in the spectral range of the Al K-shell lines above 1 keV [6,18].

For the comparison of the experimental Fe and Ho data with theory we have converted the measured transmission into the mass absorption coefficient and have plotted it in Fig. 4. (This conversion has not been made for Al because of the larger uncertainties due to the small transmission in some

spectral regions.) The given experimental error is caused by the limited accuracy of the transmission measurement and of the areal mass density of the sample. For Fe Fig. 4(a) exhibits the results of OPAL at $T=22$ eV ($\rho=0.01$ g/cm^3) which value was inferred from the Al sample. It is seen that OPAL reproduces quite well the measured spectral dependence with the trend to be slightly larger (by a factor of ≈ 1.5). The temperature in the Fe sample may be slightly different from that in the Al sample. To see the effect of a changed temperature, we plotted in Fig. 4(a) the OPAL result at $T=24$ eV, too. With this higher temperature the mean ionization increases from 6.6 to 7.0 and the mass absorption coefficient decreases in the region 75 eV $\leq h\nu \leq 110$ eV coming here closer to the experimental values.

The Ho absorption in Fig. 4(b) is in good agreement with STA when we use a larger density value ($\rho=0.03$ g/cm^3) and a smaller temperature ($kT=20$ eV) resulting in a calculated mean ionization of 7.5. We find good agreement in the low energy part of the spectrum at $h\nu \leq 150$ eV which is mainly due to bound-free transitions and to a minor degree by bound-bound transitions (they are causing the small modulations seen in the calculation in this range). At $h\nu \geq 150$ eV the prominent $4d$-$4f$ absorption feature is present in the STA calculation at the correct energy, but in the experiment it is a factor of 2 broader than in the calculation. This is attributed to the approximations used by STA to calculate the supertransition arrays, for example in the treatment of the configuration interaction [19]. We note that the detailed shape of the $4d$-$4f$ absorption band in Ho influences the value of the Rosseland mean opacity, in particular, when the temperature is larger than in the present case and the maximum of the Rosseland weight function is in the range of the $4d$-$4f$ peak.

In conclusion, we have measured spectrally resolved extreme uv opacities in Al, Fe, and Ho in the range 70 to 280 eV by using the high power laser ASTERIX IV at an energy output of about 200 J. By studying the samples at a rather low temperature of ≈ 22 eV, we could keep the background due to self-emission on a negligible level which resulted in accurate transmission data. The experimental data have been used for a comparison with the opacity models OPAL for Al and Fe and STA for Ho. The agreement between measured and calculated absorption coefficient is encouraging. Major discrepancies are present in the shape of the Ho $4d$-$4f$ absorption band which is of importance for the Rosseland mean opacity.

This work was supported in part by the commission of the European Communities in the framework of the Euratom-IPP association.

[1] F. J. Rogers and C. A. Iglesias, Science **263**, 50 (1994).
[2] R. L. Kauffman, L. J. Suter, C. D. Darrow, J. D. Kilkenny, H. N. Kornblum, D. S. Montgomery, D. W. Phillion, M. D. Rosen, A. R. Theissen, R. J. Wallace and F. Ze, Phys. Rev. Lett. **73**, 2320 (1994).
[3] A. Rickert, J. Quant. Spectrosc. Radiat. Transfer **54**, 325 (1995).
[4] S. J. Davidson *et al.*, Appl. Phys. Lett. **52**, 847 (1988).
[5] J. Bruneau *et al.*, Phys. Rev. A **44**, R832 (1991).
[6] T. S. Perry *et al.*, Phys. Rev. Lett. **67**, 3784 (1991).
[7] J. M. Foster *et al.*, Phys. Rev. Lett. **67**, 3255 (1991).
[8] L. B. DaSilva *et al.*, Phys. Rev. Lett. **69**, 438 (1992).
[9] P. T. Springer *et al.*, Phys. Rev. Lett. **69**, 3735 (1992).
[10] W. Schwanda, K. Eidmann, and M. C. Richardson, J. X-Ray Sci. Technol. **4**, 8 (1993).
[11] E. B. Saloman, J. H. Hubbel, and J. H. Scofield, At. Data Nucl. Data Tables **38**, 1 (1988).
[12] G. Winhart, dissertation, Technische Universität München, 1995 (unpublished).
[13] R. Ramis, R. F. Schmalz, and J. Meyer-ter-Vehn, Comput. Phys. Commun. **49**, 475 (1988).
[14] K. Eidmann, Laser and Particle Beams **12**, 223 (1994).
[15] I. B. Földes *et al.*, Phys. Rev. E **50**, R690 (1994).
[16] F. J. Rogers, C. A. Iglesias, and B. G. Wilson, Astrophys. J. **397**, 717 (1992).
[17] A. Bar-Shalom, J. Oreg, and W. H. Goldstein, J. Quant. Spectrosc. Radiat. Transfer **51**, 27 (1994).
[18] C. A. Iglesias *et al.*, J. Quant. Spectrosc. Radiat. Transfer **51**, 125 (1994).
[19] The shape of the measured $4d$-$4f$ peak can be calculated by detailed configuration accounting which, however, requires a huge computational effort [D. Kilcrease and J. Keady (private communication)].

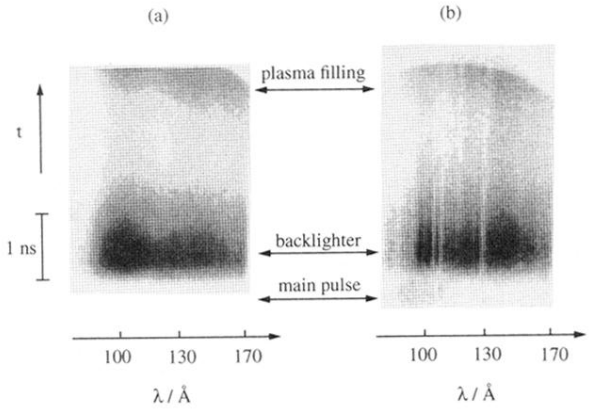

FIG. 2. Streak camera signals of the backlighter observed through a heated cavity (a) without a sample and (b) with an aluminum sample.

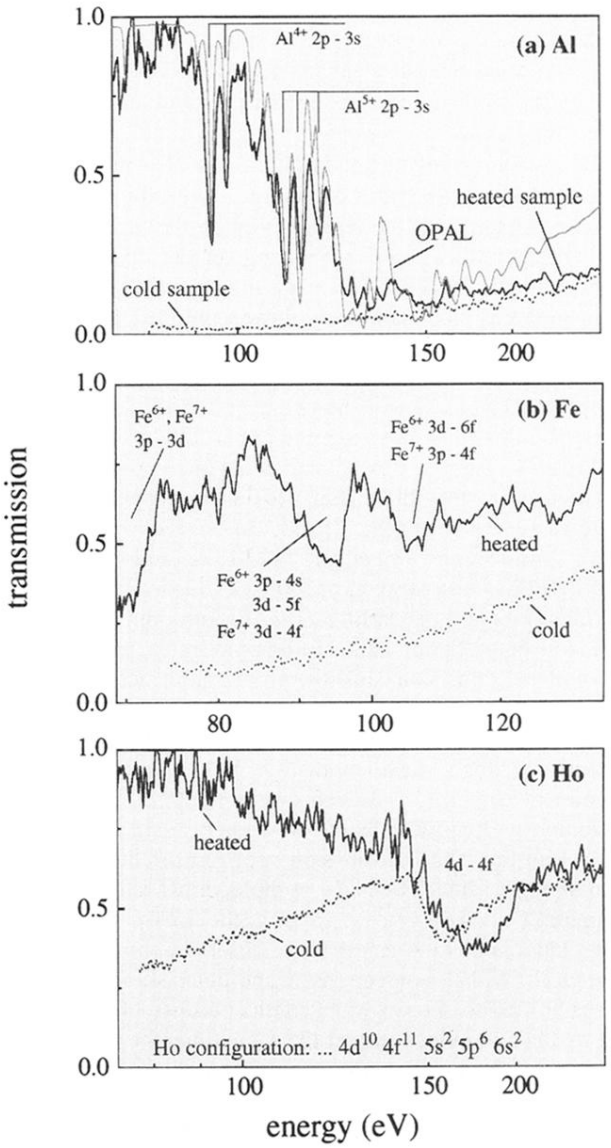

FIG. 3. Measured transmission spectra of (a) aluminum, (b) iron, and (c) holmium for the heated and cold sample, respectively. For Al (a) also a comparison with the OPAL code at $\rho = 0.01$ g/cm^3 and $T = 22$ eV is shown (the OPAL data have been shifted by 3 eV to lower photon energies for an optimum coincidence between the measured and the calculated spectra).

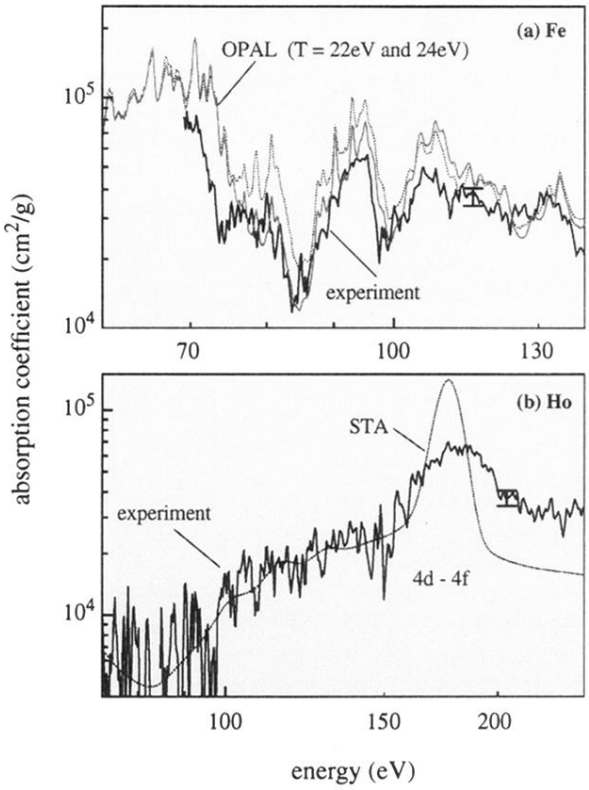

FIG. 4. Measured and calculated mass absorption coefficient versus photon energy for Fe (a) and Ho (b). In the calculations we used for Fe: $\rho = 0.01$ g/cm^3 at $T = 22$ eV (dotted) and $T = 24$ eV (grey); and for Ho: $\rho = 0.03$ g/cm^3, $T = 20$ eV.